Responses to Referee #2:

The response by Li et al. addressed this reviewer's comments in a point-by-point manner. While the authors had adequately addressed many of my comments, this reviewer feels that the authors have not fully addressed several main comments. To increase the clarity of the paper, and the validity of the results, I suggest that the authors addressed the comments below.

Response: We highly appreciate the valuable suggestions by the reviewer, which are helpful for us to improve the quality of our manuscript. We have carefully addressed the comments in point-by-point form as shown below. Detailed responses to the comment are highlighted in blue, and the revised text is _underlined in italics_. Attached please also find the marked-up manuscript with tracked changes in the revised manuscript.

2 General Comments

• Reviewer Point 3: I suggest that the authors start their conversation about the size distributions on Line 270, with their caveat that starts on Line 293. As it stands, the authors discuss the size distributions as if the SPAMS size distribution is quantitative–but it largely depends on the SPAMS detection efficiency as a function of size. The authors do segue into a conversation about the number fractions as a function of size, which is much more valid. The authors slide back into using the SPAMS size distribution again starting on Line 285, which again, without a quantitative sizing instrument is hard to interpret. Finally, the authors reference Figure S10a and S10b, but the current supplemental does not contain any figures with size distributions.

Response: Suggestion taken. The statement has been revised as follows.

Line 305-313
"Compared with the total particle size distribution, the peak values of the six main particle types show minor differences (< 80 nm) during the two different episode periods (Fig. 11b,c). However, the percentage of the six particle types distribute in wider size ranges during E2 than during E1 possibly due to the more intensive atmospheric aging. Similarly, during the two episodes (Fig. 3b,c), the relatively high fraction of the rich-K and BB particles are more affected by the primary emissions when their peak value concentrate at < 300 nm, and > 300 nm are more related to the aging process (Li et al., 2022b; Bi et al., 2011). Relatively greater fluctuation for the large-size fractions (> 1.1 µm) could be explained by the low particle concentration (a number less than 20)."

Additionally, sorry for the confusion that the previous supplemental information possibly uploads unsuccessfully. I will upload all materials more carefully this time.

The previous versions of Figure S11 (a,b) are shown in Figure R1 below.
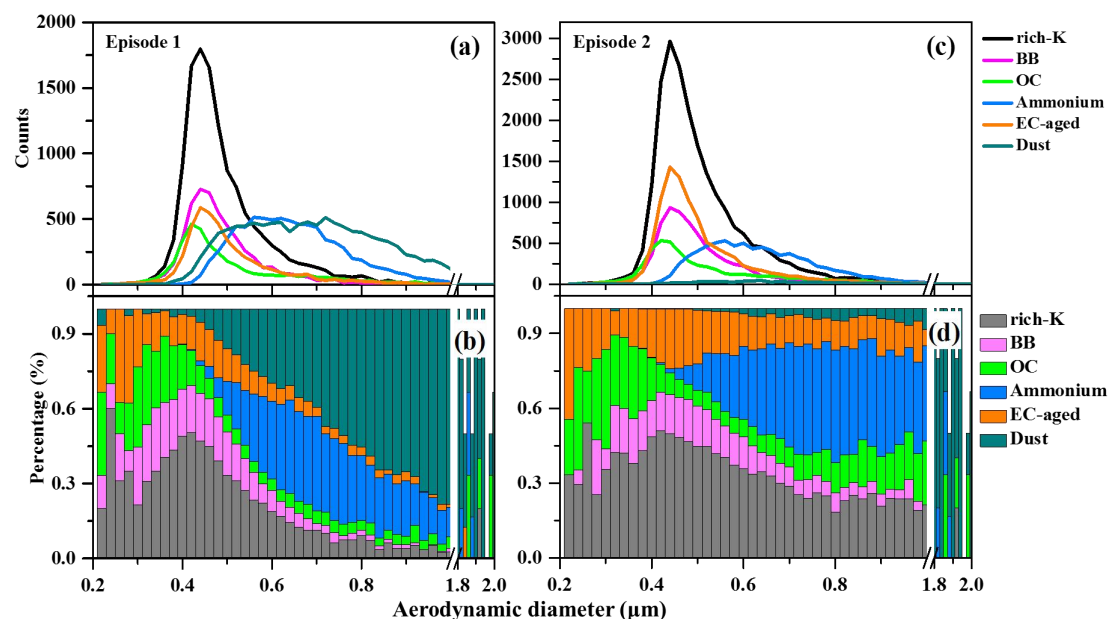

Figure R1. Size distributions of the (a, c) number concentrations and (b, d) fractions of the major six particle types (rich-K, BB, OC, Ammonium, EC-aged, and Dust) during two episodes of (a, b) E1 and (c, d) E2.

Under the reviewer's suggestion, in order to more clearly illustrate the characteristics of particle size distribution, we have replaced the figures in the current main text (Figure 3 in follows) and supplemental (Figure S10 in follows) respectively, because the number fraction is more valid.
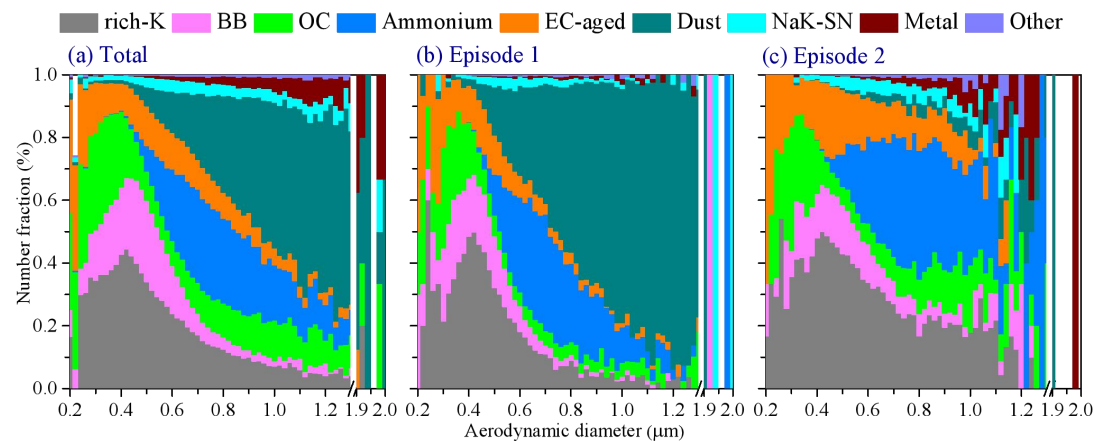

Figure 3. Size distributions of the relative number fraction (%) of the total particles for nine groups during (a) the total sampling campaign and two episodes of (b) E1 and (c) E2.
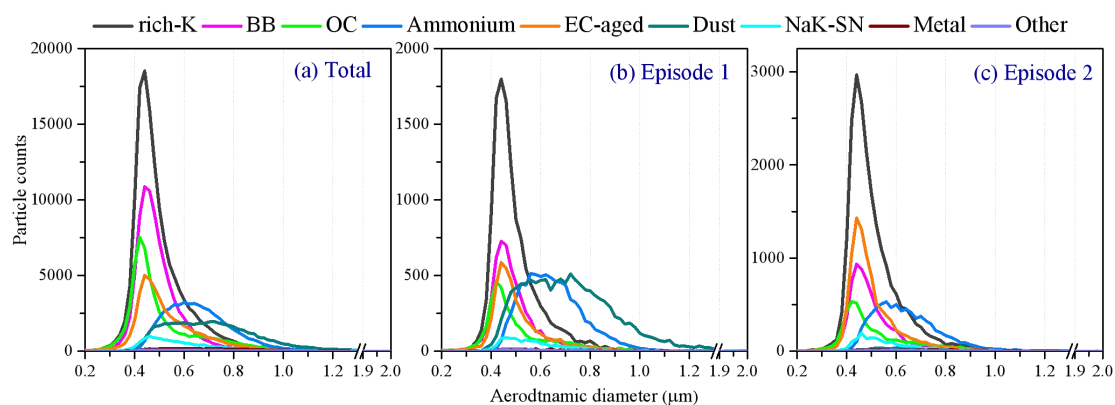
Figure S11. Size distributions of the number concentrations of the nine particle types during (a) the total observation periods and two episodes of (b) E1 and (c) E2.

• **Reviewer Point 4:** While the authors have pointed the reviewer to additional information about the rich-K particles in the supplemental material, I would like to see the authors add a description of the rich-K particles to the main text. As currently written, the text suggests that the rich-K are one type of particle from a particular source. The supplemental information, however, suggests that the particles are from different sources (biomass burning, traffic emissions, and secondary sources). Thus, it seems like there is a disconnect in using rich-K particles in the back trajectory cluster analysis. If this one particle type has different sources, then it seems like their relative fractions in the back trajectories could have several causes. Thus, this reviewer suggests that the authors clarify why they use this one cluster for particles with several sources–perhaps they have one distinct source in that they're anthropogenic? Finally, this reviewer is also surprised that potassium aerosol is formed in secondary reactions. I think this needs further explanation in the main text.

Response: Previous studies have shown that the source of rich-K is complex, which includes biomass burning, secondary formation, industrial emission, and traffic emission (e.g., Pratt et al., 2011; Bi et al., 2011; Shen et al., 2017; Zhang et al., 2017). According to the characteristics of mass spectrum (e.g., the existence of $^{79}PO_3^-$ signal indicates the sources of traffic emission) and diurnal variation (e.g., similar with BB), we point out that traffic emission and biomass burning are contributed to the chemical component of rich-K type. The coexistence strong signals of sulfate (m/z $^{97}HSO_4^-$) and nitrate (m/z $^{46}NO_2^-$ and $^{62}NO_3^-$) in the negative mass spectrum indicate that rich-K particles have undergone a certain degree of atmospheric process or affected by secondary formation. By analyzing the correlation between seven variables (Fig. S4), rich-K type is strongly correlated with Ammonium (r=0.84) and EC-aged (r=0.90) types, then well correlated with OC (r=0.70) and BB (r=0.68) types. These results further demonstrate that rich-K particle is sourced from traffic emission and biomass burning, and affected by secondary formation during the atmospheric aging.

Because the SPAMS itself is sensitive to potassium ($^{39}K^+$), in some cases, the $^{39}K^+$ signal has weak indicative. Therefore, other components (except for $^{39}K^+$) are usually combined to indicate the potential sources of specific particles. For example,

in addition to $^{39}K^+$, the biomass burning emissions also need to contain levoglucosan fragments ($^{45}CHO_2^-$, $^{59}C_2H_3O_2^-$, $^{71}C_3H_3O_2^-$, $^{73}C_3HO_3^-$) and $^{113,115}K_2Cl^+$ signals, etc., so as to further prove its accurate source. It should be emphasized that secondary formation only means that the particle type contains the abundance of sulfate and nitrate signals in its negative mass spectrum, and has no other obvious components except potassium.
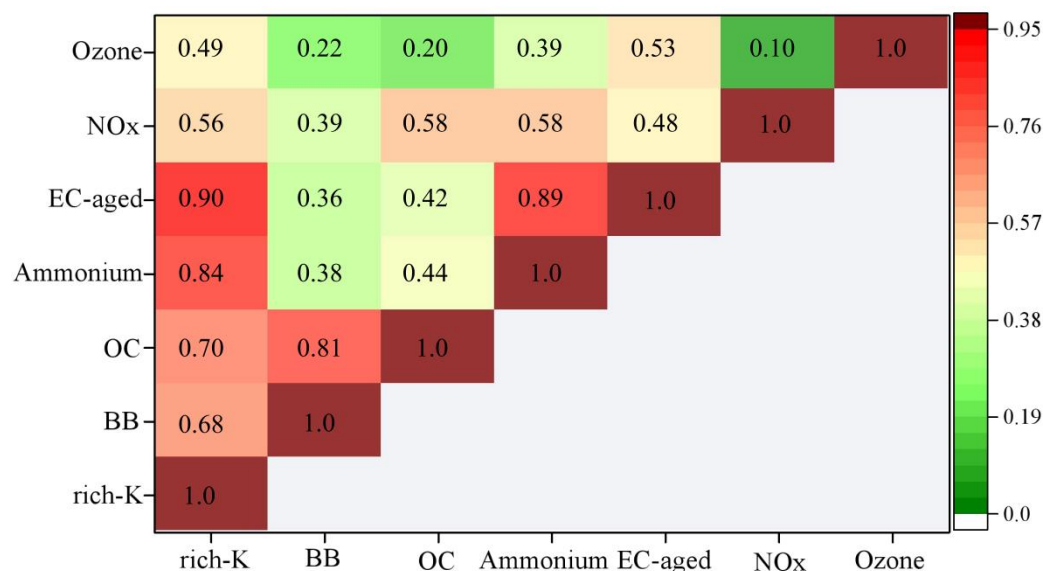

Figure S4. The correlation results between seven variables ($p < 0.01$) was statistically analyzed by IBM SPSS software (version 23). The values in the figure represent Pearson's r.

According to the reviewer's suggestion, we have added the following explanations to the main text.

Line 190-191
"Their characteristics of mass spectrum and possible sources are described in supplemental information of text S1 in detail."

Line 193-202
"Combined with the previous studies and the characteristics of the mass spectrum (Fig. S3) in this study, the rich-K particles are contributed by biomass burning and traffic emission, because that extensive works usually identify abundant $^{39}K^+$ signal for biomass burning (Pratt et al., 2011; Chen et al., 2017), while the presence of phosphate (m/z $^{79}PO_3^-$) indicates the vehicle exhaust (Yang et al., 2017). The results of the correlation between seven variables (Fig. S4) show that rich-K type was strongly correlated with Ammonium (r=0.84) and EC-aged (r=0.90) types, follow well correlated with OC (r=0.70) and BB (r=0.68) types, further demonstrate that rich-K particles type is from traffic emission and biomass burning, and is affected by secondary formation during the atmospheric aging in southeastern TP."

Line 243-250

"Cluster 3 and 4 have the comparable contributions of OC (15.5% and 12.5%, respectively), increased of BB (19.3% and 26.8%, respectively) and decreased of rich-K (26.8% and 25.2%, respectively), Ammonium (10.4% and 7.7%, respectively) and EC-aged (7.7% and 6.3%, respectively), to those of Cluster 1, but with a high contribution of Dust (16.6%), which refer Cluster 3 and 4 to as dust and biomass burning pollution. However, Cluster 1 is more influenced by compound pollution, mainly including secondary formation, biomass burning, and traffic emissions."

Line 253-254
"A stable diurnal variation of rich-K fraction is mainly due to its large proportion and diverse sources."

Reference:

Chen, Y., Wenger, J. C., Yang, F. M., Cao, J. J., Huang, R. J., Shi, G. M., Zhang, S. M., Tian, M., and Wang, H. B.: Source characterization of urban particles from meat smoking activities in Chongqing, China using single particle aerosol mass spectrometry, Environ. Pollut., 228, 92–101, https://doi.org/10.1016/j.envpol.2017.05.022, 2017.

Pratt, K. A., Murphy, S. M., Subramanian, R., DeMott, P. J., Kok, G. L., Campos, T., Rogers, D. C., Prenni, A. J., Heymsfield, A. J., Seinfeld, J. H., and Prather, K. A.: Flight-based chemical characterization of biomass burning aerosols within two prescribed burn smoke plumes, Atmos. Chem. Phys., 11, 12549–12565, https://doi.org/10.5194/acp-11-12549-2011, 2011.

• **Reviewer Point 8/9:** To this reviewer, the results in Figures R6 and R7 seem to contradict the results in Figures 6 and 7, respectively. Figure R6 suggests that higher Ox concentrations lead to higher secondary-aerosol peaks. Similarly, in Figure R7, higher RH leads to higher secondary peaks. In some cases, the opposite conclusions are reached using Figures 6 and 7. Finally, the authors should clarify that these results are speculative, because the current Ox and RH conditions are not an indicator of the past Ox and RH conditions that a particle has experienced.

Response: As the reviewer said, Figures R2 and R3 suggest that higher Ox concentrations and RH values lead to higher peak areas of secondary species. Generally, the increase in secondary component concentration is accompanied by the increase in total particle concentration. Thus, it should be explained that the increase in the total particles may be affected by the primary emission and meteorological conditions (such as regional transport) (Fig. S10 and S13). The increased trend of the ratio of each secondary species to the total particles effectively indicates that the secondary species have more formation. For all that, the current results and interpretations are speculative, because ① SPAMS only be qualitatively analyzed the individual particles information rather than quantitatively interpreted due to the limited detection rate; ② the current O_x and RH conditions are not an indicator of the past O_x and RH conditions that a particle has experienced. After taking the reviewer's suggestion, the statement has been revised as follows.

"The oxidant O_x (O_3 + NO_2) concentration and RH <u>usually</u> serve as indicators of the degree of photochemical oxidation (Wood et al., 2010) and aqueous-phase reaction (Ervens et al., 2011), receptively, <u>though the current O_x and RH conditions obtained using the in-situ measurement are not indicative of the past conditions experienced by the particle. Thus,</u> the relative number fractions of <u>$^{43}C_2H_3O^+$, $^{89}HC_2O_4^-$, $^{62}NO_3^-$, $^{97}HSO_4^-$</u> and $^{18}NH_4^+$-containing particles to the total detected particles were selected to <u>provide a rough speculative of the secondary formation mechanism in TP ambient conditions (Liang et al., 2022).</u>"

"<u>Although the detailed formation pathways and their percentage contributions to secondary species are not quantitatively estimated in this study, our results have important implications for the various possibilities affecting the characteristic of chemical components, size distribution, mixing states, and formation mechanism of aerosols in the southeast TP. More depth investigations concerning the evolution mechanisms of secondary aerosols are encouraged since TP is a significant regulator to global climate change.</u>"
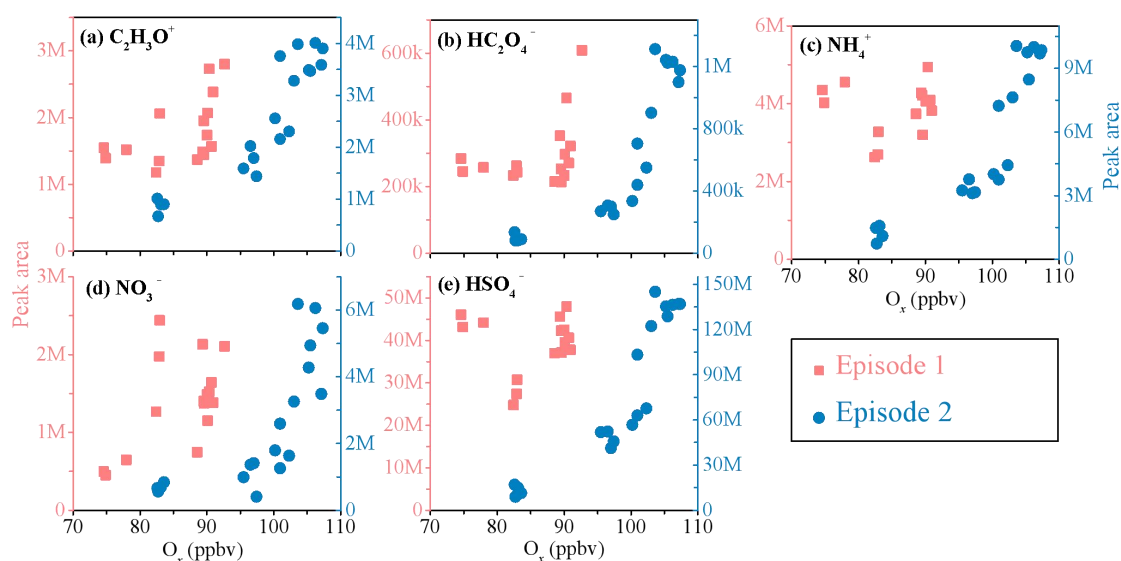

Figure R2. Correlations between the peak area (PA) for five secondary ions and O_x concentration during Episodes 1 and 2. The k and M represents thousands and ten thousands in the y-axis, respectively.
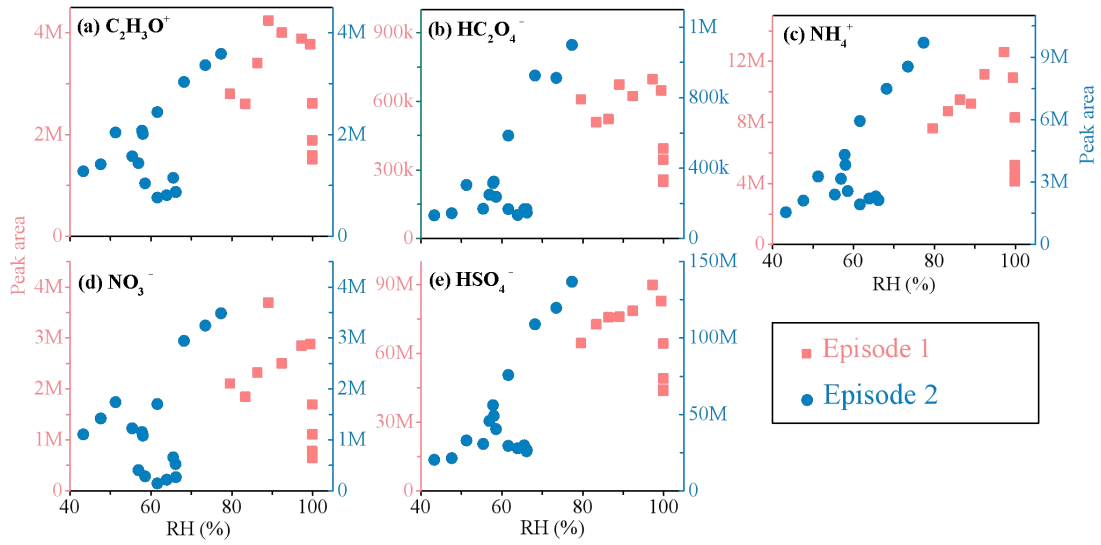
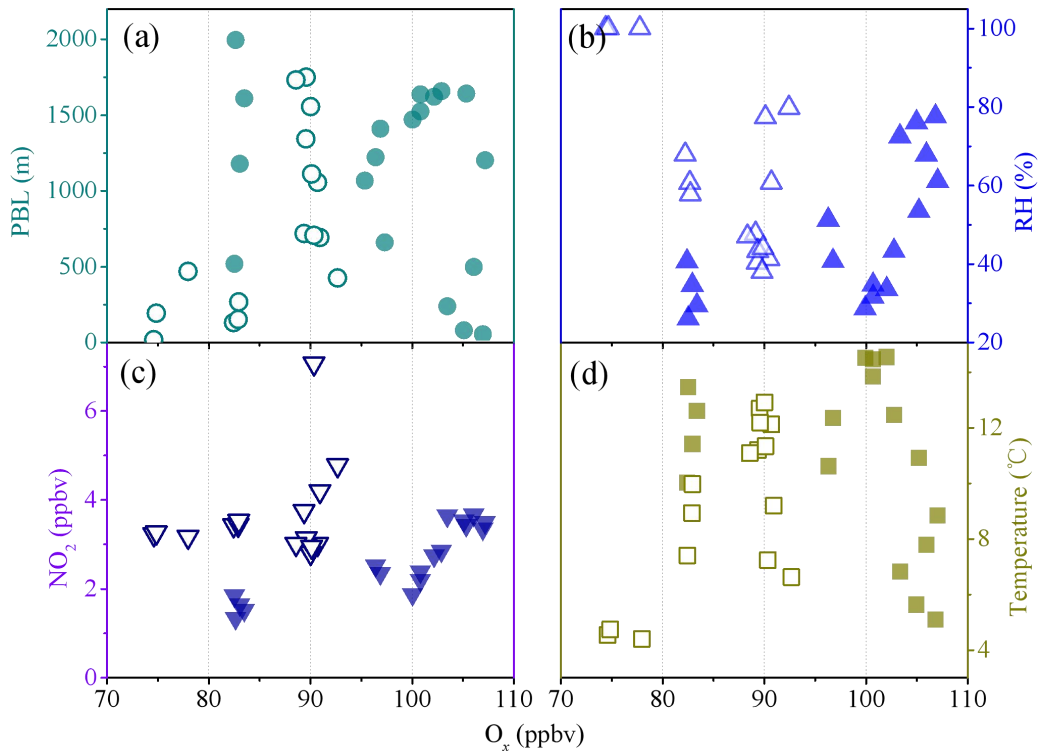Figure R3. Correlations between the peak area (PA) for five secondary ions and RH during Episodes 1 and 2.

Figure S10. Correlations between oxidant (O_x) concentration and (a) PBL, (b) RH, (c) NO_2 concentration and (d) temperature during the Episode 1 (the open shape) and Episode 2 (the solid shape).
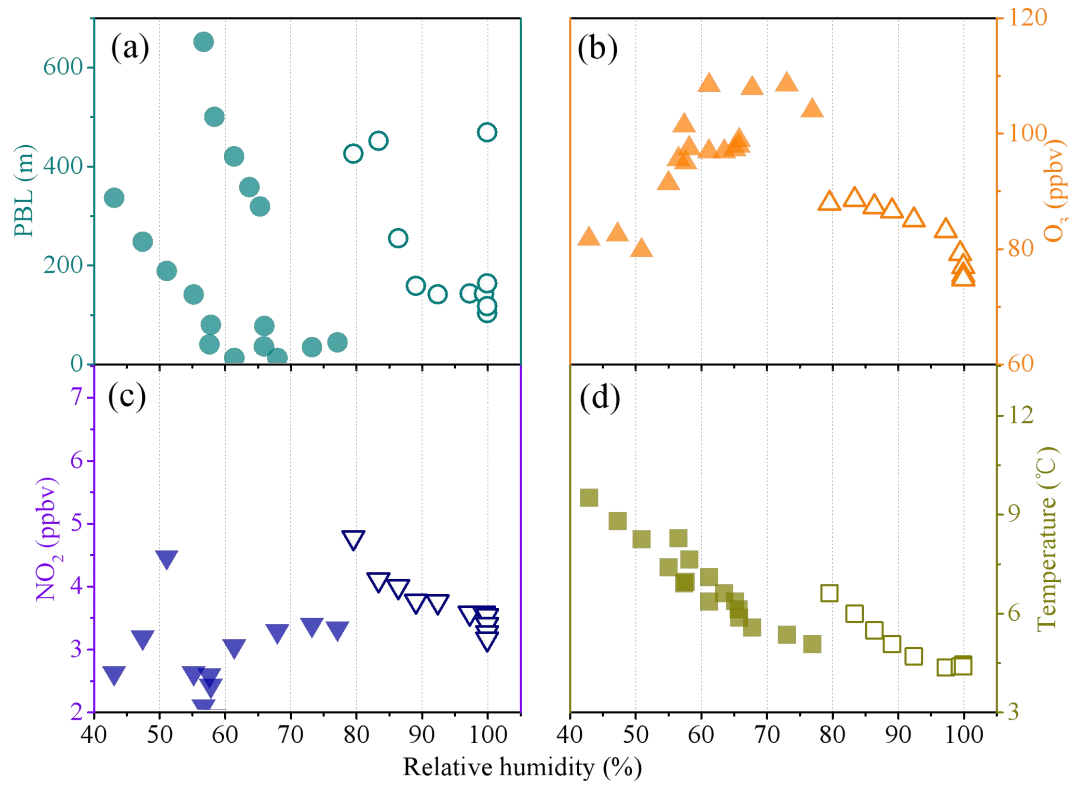
Figure S13. Correlations between RH and (a) PBL height, (b) O₃ concentration, (c) NO2 concentration and (d) temperature during the Episode 1 (the open shape) and Episode 2 (the solid shape).